Clinical Chemistry 47:8
1451–1457 (2001)

Automation and Analytical Techniques

Simultaneous Multianalyte ELISA Performed on a Microarray Platform

Rick Wiese,[1*] Yuri Belosludtsev,[1] Tom Powdrill,[1] Patricia Thompson,[2] and Mike Hogan[1]

Background: **A logical progression of the widely used microtiter plate ELISA is toward a protein array format that allows simultaneous detection of multiple analytes at multiple array addresses within a single well. Here we describe the construction and use of such a multiplex ELISA to measure prostate-specific antigen (PSA), α_1-antichymotrypsin-bound PSA (PSA-ACT), and interleukin-6 (IL-6).**

Methods: **We silanized glass plates and printed the appropriate capture antibodies to allow for the construction of "sandwich" ELISA quantification assays. We examined specificity of the assay for appropriate antigen, assembled calibration curves, and obtained PSA concentrations for 14 human serum samples. We compared the serum PSA concentrations derived through the use of our array with values obtained independently using a standard ELISA method.**

Results: **R^2 values generated by our microarray for the PSA and PSA-ACT calibration curves were 0.989 and 0.979, respectively. Analyte concentrations used for the construction of these curves were 0.31–20 μg of protein/L of diluent. IL-6 calibration curve concentrations were 4.9–300 ng of IL-6/L of diluent. The R^2 value for the IL-6 calibration curve was 0.983. The 14 human serum samples screened by this micro-ELISA technique for PSA concentrations generated a regression equation (linear) with a slope of 0.83 ± 0.10 and intercept of 0.74 ± 0.70 (R^2 = 0.88).**

Conclusions: **Multiplexed ELISA arrays are a feasible option for analyte quantification in complex biologic samples.**

Protein quantification is an indispensable tool in clinical and research laboratories. Classic ELISA is a useful tool for this quantification, but problems arise when limited sample is available and quantification of multiple antigens is desired. The microarray is one tool that would potentially fill this need for simultaneous multiparametric analysis of a biologic sample. Microarrays are widely used in genotyping and gene expression experiments *(1–3)* and readily adaptable to protein work. Previous work has explored the use of microarrays *(4–10)* and time-resolved fluorometry for multianalyte immunoassay *(11–14)*, demonstrating the utility of these methods in protein analysis. Here we demonstrate the utility of a microarray platform that exhibits detection ranges similar to classic ELISA and allows for multiple measures of multiple targets within a single well. This platform is based on a "sandwich" ELISA format and consists of titration of capture antibody concentrations printed on a glass surface, allowing for the detection of several discreet antigens by enzyme-linked fluorescence. The capture-antibody titration design is used to extend the detection range of each array well by providing lower density probe elements for quantification when saturation occurs at higher density elements.

The protein targets selected for this work were as follows: prostate-specific antigen (PSA),[3] PSA bound by α_1-antichymotrypsin (PSA-ACT), and interleukin-6 (IL-6). These proteins are recognized, particularly PSA, as serum markers of prostate health and indicators of prostatic cancer *(15–18)*. Calibration curves were prepared with purified proteins derived from human seminal fluid (PSA and PSA-ACT) or human recombinant proteins (IL-6).

Our micro-ELISA format was capable of generating calibration curves with high correlation coefficients within reference values for physiologic serum concentrations for the tested proteins (reference values similar to those used on commercially available ELISA reagent sets).

[1] Genometrix, Inc., 2700 Research Forest Dr., The Woodlands, TX 77381.
[2] University of Texas, MD Anderson Cancer Center, Houston, TX 77030.
*Author for correspondence. Fax 281-465-5002; e-mail rwiese@genometrix.com.

Received January 11, 2001; accepted May 11, 2001.

[3] Nonstandard abbreviations: PSA, prostate-specific antigen; PSA-ACT, α_1-antichymotrypsin-bound PSA; and IL-6, interleukin-6.

Human serum samples tested for PSA concentrations by our micro-ELISA demonstrated the utility of this assay as a potential diagnostic tool. These results indicate that this micro-ELISA format is applicable for the quantitative immunodetection of several antigens in parallel within a single well.

Materials and Methods

GLASS PLATE PREPARATION AND ARRAY MANUFACTURING

Standard Genometrix 96-well glass plates were cleaned and silanized according to procedures published previously *(19)*. Arrays were printed on prepared plates with the Genometrix capillary printer [discussed in Ref. *(4)*]. For this work, an 8 × 8 print head was used; this print head deposits microarray elements of ~250 pL in 250-μm spots at 300 μm center-to-center spacing. The general design of our micro-ELISA sandwich assay is illustrated in Fig. 1. The layout of the 8 × 8 array of printed antibody, one array per well in a standard 8 × 12 (96-well) microtiter format, is illustrated in Fig. 2. This 64-element array contains a 5-element capture antibody dilution series printed in duplicate for both forms of PSA and a 4-element series printed in duplicate for IL-6. Print solutions consisted of appropriate monoclonal capture antibodies diluted in print buffer [0.1 mmol/L carbonate buffer (pH 9.5) and 50 mL/L glycerol], leading to print concentrations of 5–500 mg/L (Fig. 2). The anti-total PSA and PSA-ACT capture antibodies were purchased from Diagnostic Systems Laboratories (cat. no. A-160) and Fitzgerald Industries International (cat. no. 10-P22), respectively. The anti-IL-6 capture antibody was purchased from Pharmingen (cat. no. 26451E). The rabbit IgG markers (cat. no. 31-RGG0; Fitzgerald) printed at a concentration of 150 mg/L in positions A1-A8, H-7, and H-8 are useful for the orientation and identification of probes within the array. The serum samples used for platform validation were purchased from US Biological, and PSA concentrations were acquired from US Biological with the use of a standard clinical PSA ELISA reagent set (Bayer).

MICRO-ELISA ASSAY

After overnight storage at 4 °C (postprinting), the arrayed wells of each glass plate were first rinsed multiple times, then blocked on a shaker plate for 1 h at room temperature in Blocker Casein (cat. no. 37528ZZ; Pierce Chemical Co.). Blocker Casein was aspirated from the wells, and 25 μL of appropriate antigen solutions [diluted in phosphate-buffered saline–100 mL/L fetal bovine serum] or serum samples were added to each of the test wells. PSA and PSA-ACT (cat. nos. 30-AP16 and 30-AP13, respectively) were from Fitzgerald Industries, and recombinant human IL-6 (cat. no. 26456E) was from Pharmingen. The array plate was placed in a humidity chamber and incubated at 37 °C for 2 h. After sample incubation, the plate was washed multiple times with Blocker Casein. Detection antibodies (25 μL/well) were applied next; these were rabbit anti-PSA and rabbit anti-IL-6 polyclonal antibodies, both purchased from Fitzgerald Industries (cat. nos. 20-PR50 and 20IR-09, respectively). The samples were incubated again at 37 °C in a humidity chamber for 1.5 h. After washing, an alkaline phosphatase-linked goat anti-rabbit secondary antibody (25 μL/well; cat. no. 31342ZZ; Pierce) was applied to probe for the detection antibodies. After incubation with the anti-rabbit antibody in saturating humidity for 1 h at room temperature, the

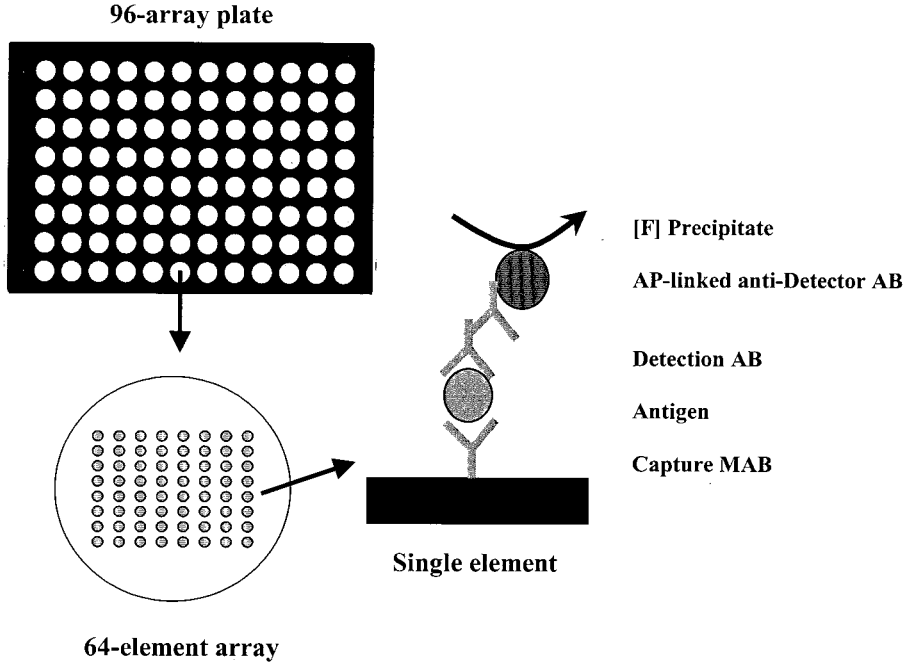

Fig. 1. Micro-ELISA general design.

Arrays (64-element) are printed into each of the 96 wells on a glass array plate. Illustrated is a single element within an array. The capture antibody (*Capture MAB*) is linked to the surface, enabling the antibody to secure free antigen. The detection antibody recognizes captured antigen, and the alkaline phosphatase-linked anti-detector antibody (*AP-linked anti-Detector AB*) recognizes bound detection antibodies. Finally, a precipitating alkaline phosphatase substrate is used to generate a fluorescent signal. *AB*, antibody; *MAB*, monoclonal AB.

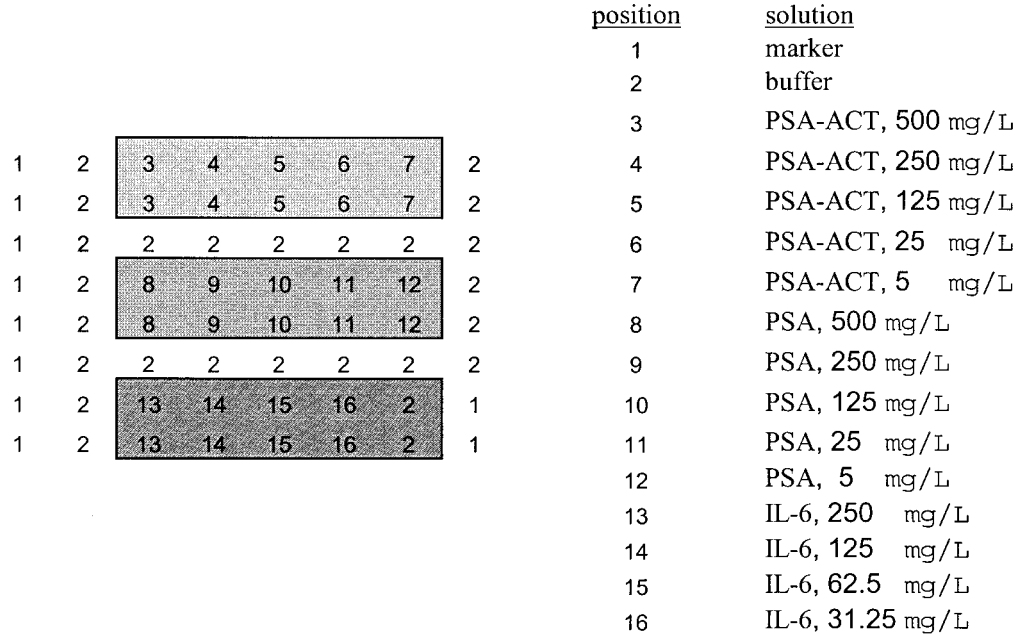

Fig. 2. Array layout.

An 8 × 8 element array is shown. For each probe (*1–16*), the appropriate print solution is listed. The marker solution contains rabbit IgG at a concentration of 150 mg/L. The buffer elements are the 100 mmol/L carbonate buffer (pH 9.5) and 50 mL/L glycerol print buffer.

plates were rinsed and the Elf®-97 (cat. no. E-6604; Molecular Probes) reagent was used to detect antigen binding according to the manufacturer's instructions.

The completed assay plate was imaged with the use of a custom-built charge-coupled device (excitation source, 345 nm; emission filter, 550 nm) camera *(4)*, controlled by custom software (Genometrix). Varying exposure time allows for the imaging of subject proteins generating signals of differing intensities. The saved images were analyzed with the use of custom spot densitometry software (Genometrix). This software automatically subtracts background from the utilized densitometry values. Spot densitometry values were used to construct densitometry vs capture antibody concentration graphs for each individual well (antigen concentration) of the calibration curve. The linear regression equations derived from each of these graphs were used to generate values corresponding to the densitometry value of the second highest capture antibody concentration (PSA antibodies, 250 mg/L; IL-6 antibody, 25 mg/L), a process that was repeated for each well (see example below). The second highest capture antibody concentration was chosen because it resides closest to the midpoint of the printed capture antibody concentrations. This procedure was followed for the densitometry data derived from each of the duplicate capture elements from each well, and the mean values obtained were calculated. As an example, in Fig. 4A, the two linear regression equations derived for the two data sets plotted are shown. For these data, the x value of 250 mg/L would be substituted into each of the regression equations, and the mean of the y values obtained would be calculated to yield the linear regression value used on the calibration curve graph at this particular antigen concentration. This process was repeated for each substrate at each concentration in each of the calibration curves, and for the determination of PSA concentrations in the tested serum samples. This process allows for increased accuracy in the quantification of analytes by the use of a maximal number of arrayed spots to generate the final plotted points on the calibration curves.

Results

An image of 16 wells is shown in Fig. 3A, which demonstrates the selectivity of the antibodies for the appropriate antigen (A1–B3), which is used to assemble the 7-point calibration curve for the three proteins of interest (C1–D3). Wells B4 and D4 were both negative controls (no recombinant protein added). As expected, in well A1 (PSA only), signal was detected only at the total PSA capture probes. In A2 (PSA-ACT), signal was detectable at both the total PSA and specific ACT-bound PSA capture probes, and in A3 (IL-6), detectable signal emanated solely from the IL-6 probes. Additionally, for each of the combinations of these substrates only those probes specific for the added antigen yielded a detectable signal (A4–B3). Wells C1–D3 were used to construct antigen titration calibration curves (Figs. 4, B–D). For each duplicate set of capture antibodies at each antigen concentration, a graph of spot densitometry value vs capture (printed) antibody concentration was plotted. An example of one of these graphs is shown in Fig. 4A. As would be expected, because these values were obtained from duplicate capture antibody sets in a single well, the graphed lines were nearly identical. The linear regression equa-

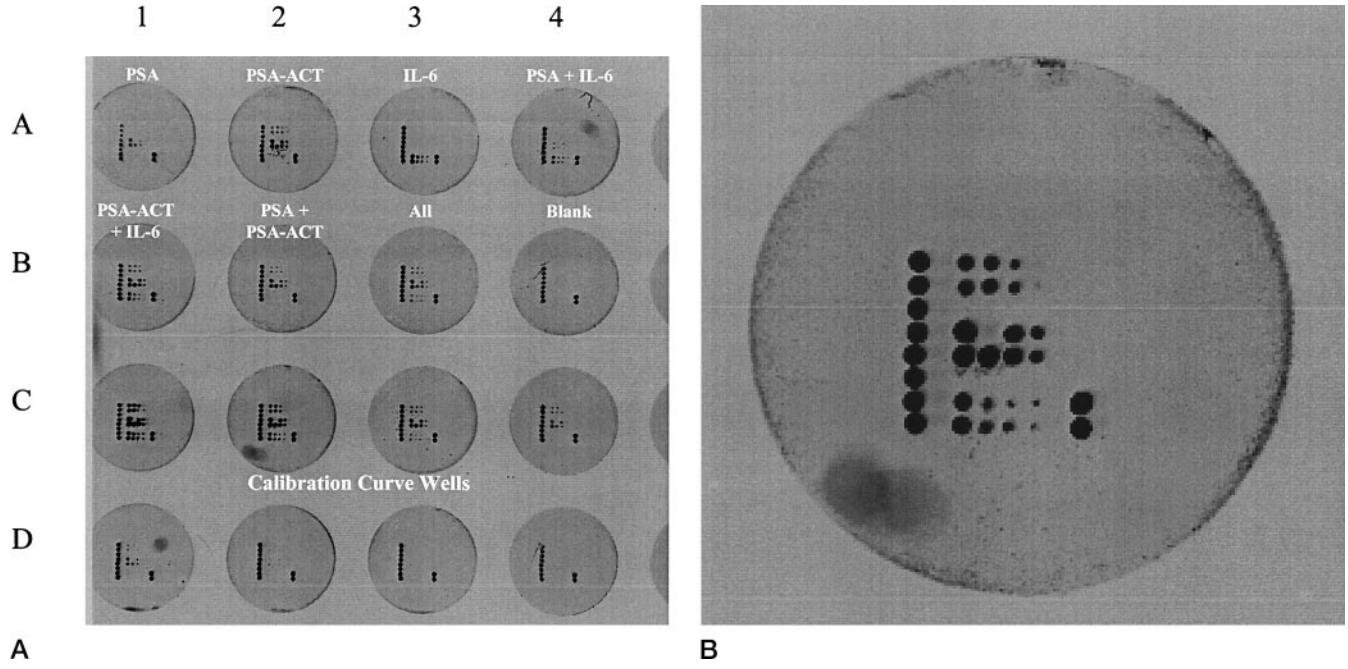

Fig. 3. Specificity of the assay (*A*) and magnified view of well C2 (*B*).

(*A*), charge-coupled device image of 16 reaction wells illustrating the specificity of the assay (*A1–B4*), as well as the calibration curve (C1–D4). Each well was incubated with 25 μL of antigen at the following concentrations: 10 μg/L PSA for well *A1*; 10 μg/L PSA-ACT for *A2*; 300 ng/L IL-6 for *A3*; 5 μg/L PSA and 150 ng/L IL-6 for *A4*; 5 μg/L PSA-ACT and 150 ng/L IL-6 for *B1*; 5 μg/L PSA and 5 μg/L PSA-ACT for *B2*; 3.33 μg/L PSA, 3.33 μg/L PSA-ACT, and 100 ng/L IL-6 for *B3*; blank for *B4*; 20 μg/L PSA, 20 μg/L PSA-ACT, and 300 ng/L IL-6 for *C1*; 10 μg/L PSA, 10 μg/L PSA-ACT, and 150 ng/L IL-6 for *C2*; 5 μg/L PSA, 5 μg/L PSA-ACT, and 75 ng/L IL-6 for *C3*; 2.5 μg/L PSA, 2.5 μg/L PSA-ACT, and 37.5 ng/L IL-6 for *C4*; 1.25 μg/L PSA, 1.25 μg/L PSA-ACT, and 18.75 ng/L IL-6 for *D1*; 0.625 μg/L PSA, 0.625 μg/L PSA-ACT, and 9.375 ng/L IL-6 for *D2*; 0.3125 μg/L PSA, 0.3125 μg/L PSA-ACT, and 4.6875 ng/L IL-6 for *D3*; and blank for *D4*.

tions derived from each of these graphs were then used to derive the points for the linear regression value vs antigen concentration graph (calibration curves) shown in Fig. 4, B–D. Microarray-derived calibration curves for PSA-ACT, PSA, and IL-6, are shown in Fig. 4, B, C, and D, respectively. For the total PSA calibration curve, the highest concentration is omitted so upper limits match on both PSA forms (PSA total concentration is the sum of PSA and PSA-ACT, so the titration curve for detectable antigen actually covers the detection range, 0.625–40 μg/L, for the total PSA antibody). The correlation coefficients of these calibration curves were comparable to those attained with the use of the standard ELISA over equivalent analyte ranges. The values obtained by the Genometrix micro-ELISA for serum PSA are illustrated in Fig. 5, which demonstrates concentrations (*x* axis) vs those reported to us by US Biological (*y* axis). A correlation coefficient of 0.88 was obtained in this comparison.

Discussion

This multiplex micro-ELISA system allows for savings of materials and time in the construction of calibration curves and the analysis of samples compared with traditional ELISA, advantages that are attributable to the fact that the calibration curves can be run simultaneously (all analytes in a single well), instead of single or replicate wells for each concentration of each antigen or sample. In addition to time and sample savings (only 25 μL of sample is needed), the use of capture antibodies is decreased in this system as well. As an example, 40 μL of the IL-6 capture antibody would be necessary to prepare one 96-well microtiter plate for the standard ELISA according to the manufacturer's recommended dilutions. Performing protein quantification by our micro-ELISA system with the use of array construction by capillary printer *(4)* makes it possible to print more than one hundred 96-well arrays with this same 40 μL of capture antibody.

The information available from each well is greater in this microarray configuration compared with a standard ELISA. In a standard ELISA, the values used to determine analyte concentration are three sample absorbance values (if the test is performed in triplicate) with one value per assay well. For the micro-ELISA, the number of data points used to determine analyte concentrations are no less than 4 (for the lowest IL-6 concentrations), up to a maximum of 10 capture-element densitometry values, and these data are obtained with the use of a single well. The use of a capture antibody dilution series allows for a greater working range in the micro-ELISA format as well. As the antigen concentration increases, lower capture antibody concentration probes are detectable, and as the higher detection probe concentrations become saturated, the lower probe concentrations can be used for quantification. This factor virtually eliminates the necessity to titrate samples and repeat an assay as in a standard ELISA. This is especially valuable when limited sample

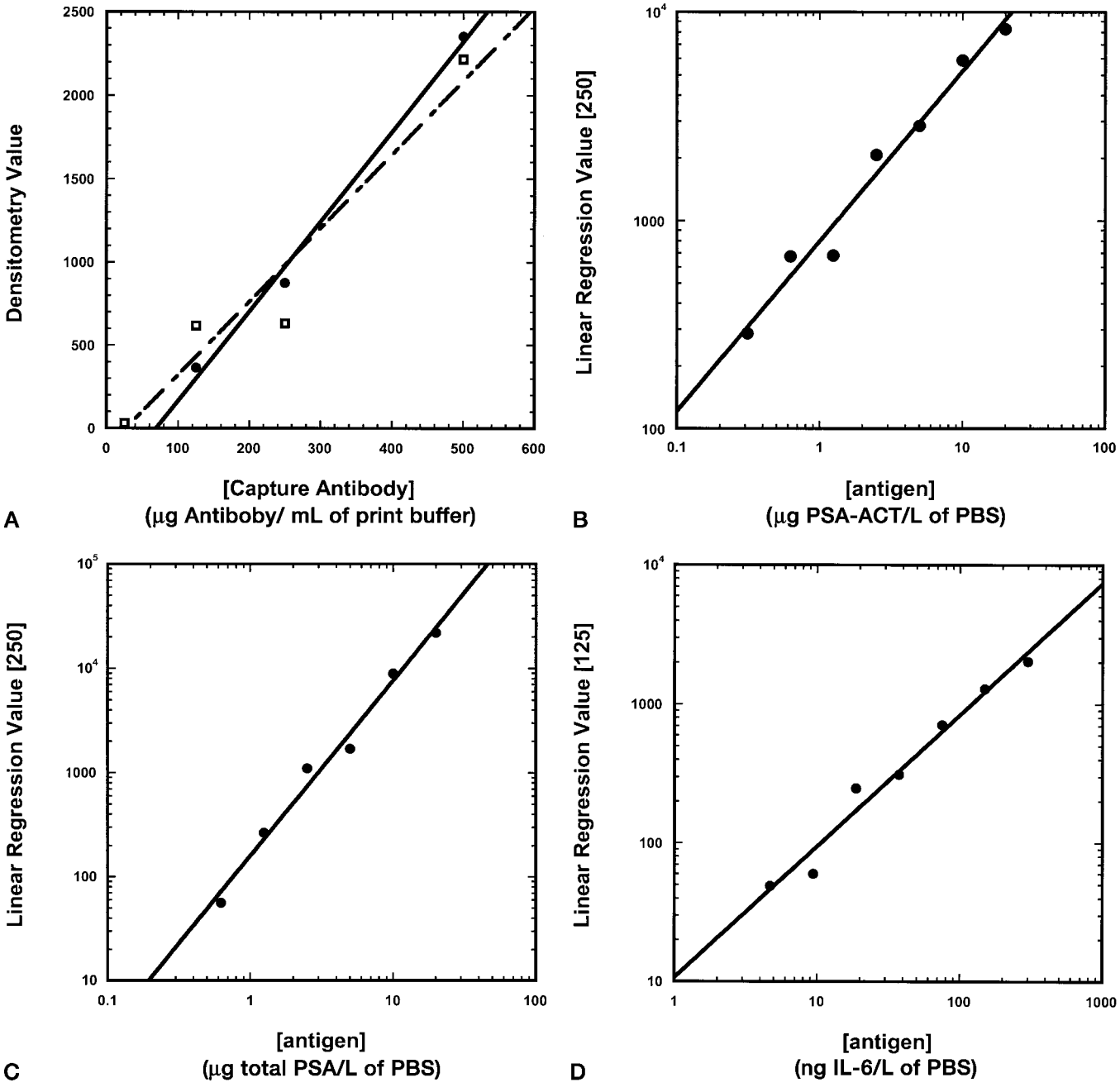

Fig. 4. Representative densitometry vs capture probe concentration graph (*A*) and calibration curves derived by the micro-ELISA for PSA-ACT (*B*), PSA (*C*), and IL-6 protein calibrators in phosphate-buffered saline (*D*).

(*A*), regression equations are shown for the duplicate measures within a single well. As outlined in *Materials and Methods*, the second highest capture antibody concentration (in this case 250 mg/L) is substituted into these regression equations (as the *x* value), and the *y* values generated by each equation are then averaged and plotted against the antigen concentration to generate the calibration curves. Equation for *solid line*: $y = -372 + 5.3851x$ ($R^2 = 0.993$); equation for *dashed line*: $y = -118.78 + 4.4135x$ ($R^2 = 0.933$). (*B*), equation for line: $y = 796.58 \times x^{0.81663}$ ($R^2 = 0.979$). (*C*), equation for line: $y = 158.77 \times x^{1.6838}$ ($R^2 = 0.989$). (*D*), equation for line: $y = 10.691 \times x^{0.9465}$ ($R^2 = 0.983$).

volumes are available. Additionally, this array design is not constrained by the need to analyze proteins present within the sample at approximately equal concentrations. In the experiments reported here, there is an ~500-fold difference in protein concentrations from the highest (PSA, 20 μg/L) to the lowest (IL-6, 4 ng/L); other work we have completed has demonstrated a range of ~500 000-fold (2 mg/L–4 ng/L) within a single well (data not shown).

The micro-ELISA is expandable to the standard array size (16 × 16 elements) typically used for production (Genometrix), a feature that would allow for the determination of 20–30 individual proteins within a single array. Polyclonal antibodies were used as detector antibodies in

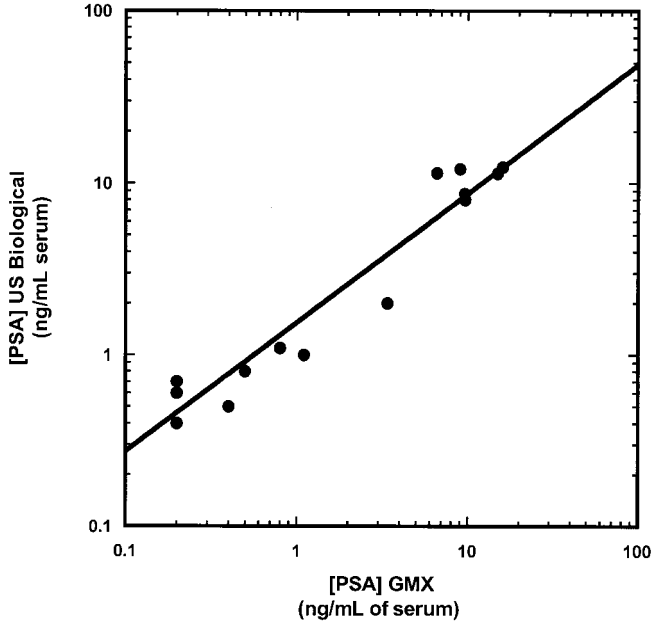

Fig. 5. Correlation graph of 14 human serum PSA concentrations as determined by Genometrix micro-ELISA (*x axis*) and independently by US Biological by the use of traditional ELISA (*y axis*).

The regression equation (linear) for these data describes a line with a slope of 0.83 ± 0.10 and intercept of 0.74 ± 0.70 (R^2 = 0.88).

this array, and no cross-reactivity was detected. Therefore, it could be hypothesized that larger arrays made entirely of monoclonal antibodies should have no problem with cross-reactivity as well (possibly polyclonal detector antibodies will not encounter problems at greater densities either, so long as monoclonal capture antibodies are used exclusively).

Another advantage of this ELISA platform is the fact that the loss of a single data point (probe value) does not negate the value of a test well. This is attributable to redundancy (capture antibodies printed in duplicate) and the use of several capture antibody concentrations. The use of regression equations formed from the titration of capture antibody has a balancing effect on occasional outlying data points without over- or underemphasizing their impact on the total set as well.

Unfortunately, the detection limit (the derived value of the signal from elements in the blank well plotted on the appropriate calibration curve) for each of these ELISA pairs could not be computed. When corrected for background, the various capture elements within the blank well gave a densitometry value of 0, yielding an infinitely low hypothetical detection limit. Additional assays performed with this array design and others in development have demonstrated a mean sensitivity of ~5 ng/L for various analytes (different detection and imaging techniques were used, allowing for sensitivity measurements; data not shown).

The comparison of results (micro-ELISA vs standard ELISA) in human serum samples serves to demonstrate the applicability of this technology. Additional validation work is planned for internal comparison on larger antibody arrays, but we thought that for this initial report, ELISA results supplied from an external source would be appropriate.

The format of this assay is the standard 96-well glass plate array used for all array work at Genometrix. This format is easily automated (genotyping and gene expression work done by Genometrix on this platform is already automated), allowing for a further increase in knowledge gained per unit of time and resources spent. This microarray format has the potential to make an impact on proteomics work, affecting researchers in all biomedical fields.

References

1. Collins FS. Microarrays and macroconsequences. Nat Genet 1999;21:2.
2. Lander ES. Array of hope. Nat Genet 1999;21:3–4.
3. Southern E, Mir K, Shchepinov M. Molecular interactions on microarrays. Nat Genet 1999;21:5–9.
4. Mendoza LG, McQuarry P, Mongan A, Gangadharan R, Brignac S, Eggers M. High-throughput microarray-based enzyme-linked immunosorbent assay (ELISA). Biotechniques 1999;27:778–88.
5. Ekins RP. Ligand assays: from electrophoresis to miniaturized microarrays. Clin Chem 1998;44:2015–30.
6. Ekins RP, Chu FW. Multianalyte microspot immunoassay-microanalytical "compact disk" of the future. Clin Chem 1991;37:1955–67.
7. Ekins RP, Chu FW. Microarrays: their origins and applications. Trends Biotechnol 1999;17:217–8.
8. Davies H, Lomas L, Austen B. Profiling of amyloid β peptide variants using SELDI proteinchip arrays. Biotechniques 1999;27:1258–61.
9. Lueking A, Horn M, Eickhoff H, Bussow K, Lehrach H, Walker G. Protein microarrays for gene expression and antibody screening. Anal Biochem 1999;270:103–11.
10. Silzel JW, Cercek B, Dodson C, Tsay T, Obremski RJ. Mass-sensing, multianalyte microarray immunoassay with imaging detection. Clin Chem 1998;44:2036–43.
11. Kakabakos SE, Christopoulos TK, Diamandis EP. Multianalyte immunoassay based on spatially distinct fluorescent areas quantified by laser-excited solid-phase time-resolved fluorometry. Clin Chem 1992;38:338–42.
12. Xu YY, Pettersson K, Blomberg K, Hemmila I, Mikola H, Lovgren T. Simultaneous quadruple-label fluorometric immunoassay of thyroid-stimulating hormone, 17 α-hydroxyprogesterone, immunoreactive trypsin and creatine kinase MM isoenzyme in dried blood spots. Clin Chem 1992;38:2038–43.
13. Luo LY, Diamandis EP. Preliminary examination of time-resolved fluorometry for protein array applications. Luminescence 2000;15:409–13.
14. Scorilas A, Bjartell A, Lilja H, Moller C, Diamandis EP. Streptavidin-polyvinylamine conjugates labeled with a europium chelate: applications in immunoassay, immunohistochemistry and microarrays. Clin Chem 2000;46:1450–5.
15. Adler HL, McCurdy MA, Kattan MW, Timme TL, Scardino PT. Elevated levels of circulating interleukin-6 and transforming growth factor-β1 in patients with metastatic prostatic carcinoma. J Urol 1999;161:182–7.
16. Jung K, Elgeti U, Lein M, Brux B, Sinha P, Rudolph B, et al. Ratio

of free or complexed prostate-specific antigen (PSA) to total PSA: which ratio improves differentiation between benign prostatic hyperplasia and prostate cancer. Clin Chem 2000;46: 55–62.

17. Jung K, Brux B, Lein M, Rudolph B, Kristiansen G, Hauptmann S, et al. Molecular forms of prostate-specific antigen in malignant and benign prostatic tissue: biochemical and diagnostic implications. Clin Chem 2000;46:47–54.

18. Weckermann D, Maassen C, Wawroschek F, Harzmann R. Improved discrimination of prostate cancer and benign prostatic hyperplasia by means of the quotient of free and total PSA. Int Urol Nephrol 1999;31:351–9.

19. Falipou S, Chovelon J-M, Martelet C, Margonari J, Cathignol D. New use of cyanosilane coupling agent for direct binding of antibodies to silica supports. Physicochemical characterization of molecularly bioengineered layers. Bioconj Chem 1999;10:346–53.